

Cooling and Roughness Effects on Transition on Nozzle Throats and Blunt Bodies

Anthony Demetriades*

Montana State University, Bozeman, Montana 59717

Observations of boundary-layer transition in a supersonic wind-tunnel nozzle throat were made in the region where the local Mach number increased from 0.4 to 2. The wall temperature ranged from adiabatic to 0.66 times the stagnation temperature, and its surface was roughened with random sand-grain, weave-type, and wire-screen roughness. It was found that wall cooling accelerates transition markedly regardless of surface conditions and that for a given height the random sand-type roughness is generally the most effective transition trigger. Transition location was much less sensitive to weave-type roughness and its orientation, although a drastic transition Reynolds number decrease was noted when the weave wavelength increased. With the roughness small or absent, phenomena involving boundary-layer relaminarization were observed. A substantial portion of these data cannot be accounted for by existing blunt-body boundary-layer transition correlations.

Nomenclature

a, b, c, d	= empirical (experimental) constants in Eq. (1)
k	= roughness height
\bar{k}	= dimensionless roughness height
M_e	= edge Mach number
p	= pressure, Torr or mm Hg abs
p_0	= stagnation pressure, Torr or mm Hg abs
p_{0B}	= stagnation pressure at the beginning of transition, Torr or mm Hg abs
q	= flow dynamic pressure, Torr or mm Hg abs
R_N	= surface radius of curvature
Re_θ	= momentum Reynolds number, $\rho_e u_e \theta / \mu_e$
$Re_{\theta T}$	= value of Re_θ at transition
S	= wavelength of roughness pattern (Fig. 2), cm
T_e	= local edge static temperature, °F
T_w	= wall temperature, °F
T_0	= tunnel stagnation temperature, °F
t	= "land area" (width) of weave-type roughness (Fig. 2), cm
u_e	= local edge flow velocity, m/s
x	= distance parallel to surface ($x = 0$ at throat), cm
α	= angle between flow vector and weave-type roughness axis, deg
θ	= boundary-layer momentum thickness, cm
μ_e	= edge fluid viscosity, P
ρ_e	= edge fluid density, kg/m ³

Introduction and Background

AMONG all high-speed boundary-layer transition phenomena debated over recent years, some consensus seems to have been reached on the data describing transition on roughened blunted objects, e.g., on the windward side of spheres or sphere cones. This consensus has been expressed by Batt and Legner¹ in the form of an empirical formula that correlates the momentum Reynolds number at transition by

$$Re_{\theta T} = a \frac{[(k/\theta)(T_e/T_w)]^b}{[1 + c(k/R_N)]^d} \quad (1)$$

The values of $a = 500$, $b = d = -1.5$, and $c = 350$ quoted by Batt and Legner resulted from their extensive survey of experiments with greatly diverse flow facilities, models, and measurement methods²⁻⁵ and are consistent with physical arguments advanced by Van Driest,⁶ Dirling et al.,⁷ and others. It is noteworthy that a good portion of the data in this survey was free of disturbing noise generated by turbulent wind-tunnel sidewall boundary layers^{2,5}; other data^{3,4} subject to this noise were rationalized by the decreased importance of the noise in the presence of the surface roughness on the experimental models.

It is the purpose of this paper to discuss two issues inherent in correlation Eq. (1), in the light of new transition measurements bearing on the size and type of roughness, and its importance relative to the surface temperature T_w . One key issue is the association of the roughness height with the inverse of T_w . The rationale here is that as T_w is lowered the boundary layer ebbs, exposing the tops of the roughness elements and in turn causing roughness-triggered transition. Wall cooling, which might otherwise suppress Tollmien-Schlichting instabilities⁸ and delay transition, thus finds itself promoting transition by effectively increasing the roughness height. Another viewpoint, however, states that roughness is not necessary for the appearance of transition on cooled blunt bodies^{9,10} and that wall cooling by itself can make the layer turbulent, perhaps by triggering instabilities not yet measured or understood, such as those related to crossflows or Goertler vortices.¹¹ To arbitrate these two diverse views, transition measurements were indicated on cooled blunt bodies with smooth walls to find the effect of T_w when $k = 0$.

The second issue raised concerned the type of roughness for which blunt-body transition correlations, in general, are valid. Reference 2 presented a comparison, predating the establishment of Eq. (1), of blunt-body transition data without accounting for curvature effects, and for random-distributed (sand-grain) roughness with k defined as an average or "significant" peak-to-valley height. Plotted in this manner, data from some key experiments, shown in Fig. 1, seem to follow correlation Eq. (1) with $a = 215$, $b = -0.7$, and $d = 0$. Random, sand-grain roughness describable by a single parameter k is, of course, idealized and, as Reda⁵ points out, quite unrealistic in materials for modern applications. A material of considerably more current interest is one with a periodic three-dimensional pattern⁵ generically known as a "weave." A second objective of this work, therefore, was to see how transition data with such a surface pattern compared with random roughness, using the random-roughness data of Fig. 1 as a point of departure.

Received Oct. 8, 1990; revision received Sept. 8, 1991; accepted for publication Feb. 4, 1992. Copyright © 1992 by the American Institute of Aeronautics and Astronautics, Inc. All rights reserved.

*Professor of Mechanical Engineering, Associate Fellow AIAA.

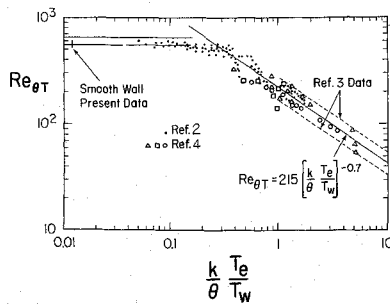


Fig. 1 Comparison of random-roughness data taken in Ref. 2 using the present nozzle technique, with data from blunt bodies.

Technique

The technique employed here was to simulate the boundary-layer growth on a blunt body with the boundary-layer growth in the sonic-throat region of a DeLaval nozzle.² Although the simulation is not exact, the sonic-throat approach has been recognized as an effective way of overcoming the great difficulties in probing boundary layers on blunt objects at supersonic and hypersonic speeds. Much of the data shown on Fig. 1, supplied by Ref. 2 using just this technique, are in good agreement with direct measurements on blunt bodies. In this figure it is already shown that deviations from the correlation (with $a = 215$, $b = -0.7$, $d = 0$) were found using this technique in the $k = 0$ limit for adiabatic walls. This paper extends the work of Ref. 2 to wall cooling and weave-type roughness.

As in Ref. 2, the flowfield was generated by the two-dimensional nozzle of the Montana State University continuous air supersonic wind tunnel. All data were taken in a converging-diverging channel of constant 3-in. (7.6 cm) width, in the middle of which the sonic-throat constriction is 0.7 in. (1.78 cm) high. The gradual throat curvature (30-cm radius), complete optical visibility, high-precision automated probe actuators, and subminiature diagnostic probes had produced detailed measurements of the laminar boundary-layer profiles and growth, reported in Ref. 2, in the range $0.4 < M_e < 2$, $100 < Re_\theta < 700$, and pressure gradient parameter $-(\theta/q)(dp/dx) > -0.0005$ (as in all other literature quoted, the momentum thickness refers to the smooth-wall condition). These conditions were obtained at different distances x from the sonic throat and over a range of the tunnel stagnation pressure p_0 . All surfaces of the channel upstream of the region where transition was generated had laminar sidewall boundary layers.

The nozzle surface temperature T_w was controlled by liquid nitrogen circulating in channels machined just under the nozzle surface and was monitored continuously by seven thermocouples located at 1-in. (2.54-cm) intervals along the nozzle centerline. The cooled section of the nozzle began 10 cm upstream of the throat and ended 10 cm downstream of it; the 10-cm distance translates, in this case, to a length equal to 110–190 throat boundary-layer thicknesses, depending on tunnel pressure. Because of the airflow, of stagnation temperature set at 115°F, T_w could be decreased only to about –100°F, and its distribution along x varied by as much as 25°F at any one setting; however, it was possible to maintain any T_w distribution constant in time within 2°F. In all data quoted later, T_w represents an average over x with an error band of about 10°F. The attainable T_w/T_0 ratios were therefore no lower than about 0.66 but, as will be seen, were able to cause substantial movement of the transition zone.

Three kinds of roughnesses were tested. Random sand-type roughness was once more utilized, but this time under wall-cooling conditions. Wire screens made of stainless steel mesh were used to simulate “weave-type” surfaces; chemical etching of brass shim stock was used to produce similar weave-type surfaces in the grid pattern shown on Fig. 2. The average peak-to-valley height k of the random sand-type roughness was defined statistically from profilometer records. For the

screens k was defined as the “knuckle” at the crossing of two wire elements and thus was twice the mesh wire diameter, and for the etched roughness k equalled the shim thickness (Fig. 2). For the screen and etched roughnesses, therefore, k was known with high precision; for the etchings, the periodicity of the pattern was characterized by an equally well-known wavelength (the quantity S in Fig. 2). All roughnesses were attached on thin, flexible sheets (“overlays”), dimensioned to span the tunnel and designed for attachment on the nozzle surface by an adhesive, covering the cooled section of the nozzle block. A total of 16 such overlays, including a perfectly smooth one and covering a k range from 0 to 0.0072 in. (0 to 0.018 cm), were constructed and tested.

Measurements

The measurement of boundary-layer transition was done with a hot-film anemometer probe, the tip of which consisted of a 0.02 in. diam (0.05 cm) Kimax glass rod sharpened into a slender wedge. A 0.02×0.004 in. (0.05×0.01 cm) platinum film, located at the stagnation line of the wedge with its long axis parallel to the surface and normal to the flow, was powered by a constant 30-mA current and was connected to an ac detection circuit with a 500-kHz passband. While the signal obtained with the film was indistinguishable from the electronic noise when the boundary layer was laminar, intense signals rich in high-frequency content were always present when the layer was turbulent. As was also done in Ref. 2, transition was detected for each particular overlay and wall and stagnation temperature by positioning the film sensor inside the boundary layer at a fixed distance x from the throat and “sweeping” the tunnel pressure p_0 over a wide range while recording the film output. By noting the p_0 levels at the beginning and end of the transition process, the $Re_{\theta T}$, k , and T_w/T_0 values were determined for this transition “event.” A total of 466 transition events were recorded for various combinations of overlay types and values of x , p_0 , and T_w , hence also for $Re_{\theta T}$, M_e , k/θ , and T_w/T_0 , including “beginning” and “end” values of $Re_{\theta T}$. By carefully throttling the nozzle coolant and monitoring the thermocouples during the p_0 sweep, it was possible to duplicate the observed transition phenomena without hysteresis due to the direction (increase or decrease) of the p_0 change.

The technique of Ref. 2 presented earlier depended on the so-called wideband detection method in the sense that for

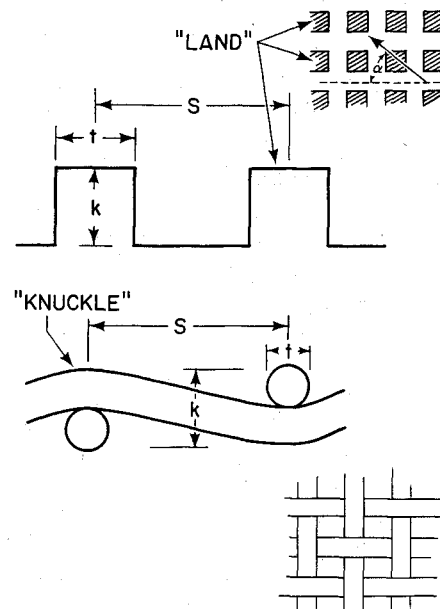


Fig. 2 Basic configuration and nomenclature of etched roughness (top) and screen roughness (bottom).

adiabatic conditions, and independent of the character of the roughness, turbulence onset occurred quite uniformly over the 0–500 kHz spectrum. When cooling was introduced in the present work, turbulence growth was found to be frequency selective, i.e., the transition process was more evident at certain frequency bands than others. Being outside the direct interests of the research, this phenomenon, which deserves a second look because of its implications in boundary-layer stability, was not pursued further; to keep the measurement reliable, a narrowband technique was also used, for the lower T_w , by which transition was detected from the study of a narrow high-frequency band behavior vs p_0 . By comparison with the wideband data, a consistent definition of transition was achieved when this band was centered at 100 kHz.

Results and Discussion

The effect of wall cooling on the smooth-wall beginning transition is shown in Fig. 3. In the region of the nozzle shown, which has a favorable pressure gradient, transition is moved upstream along the nozzle as T_w decreases. This effect was also observed without exception for all added roughness regardless of its type or height. In fact, observations of the transition Reynolds number $Re_{\theta T}$ vs random-roughness height k , made at later stages of the experiment and shown on Figs. 4 and 5, confirm this finding by the obvious extrapolation of the data to $k = 0$. It therefore appears that the presence of roughness is not a requirement for explaining why cooling moves the transition zone upstream. As mentioned in the Introduction, this effect of wall cooling has been observed by numerous investigators^{4,12,13} on blunt bodies; the cooled nozzle surface once more behaves similarly despite its imperfect simulation of blunt-body flow and the possibility of instabilities inherited from upstream regions of the tunnel circuit.

Lysenko and Maslov¹⁴ have suggested that transition on smooth-wall models internally cooled to low T_w during wind-tunnel measurements may be due to ice particles forming on and "roughening" the surface. Among the early observers of cooling-induced transition on blunt bodies, Cooper et al.¹⁵ carefully considered and rejected the possibility of surface

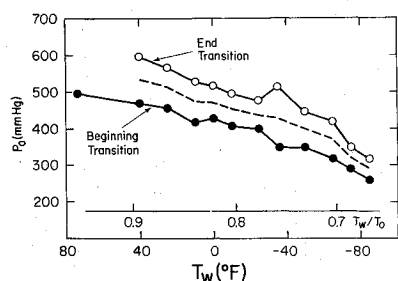


Fig. 3 The smooth-wall temperature dependence of the tunnel stagnation pressures at which transition was noted, near the nozzle sonic point.

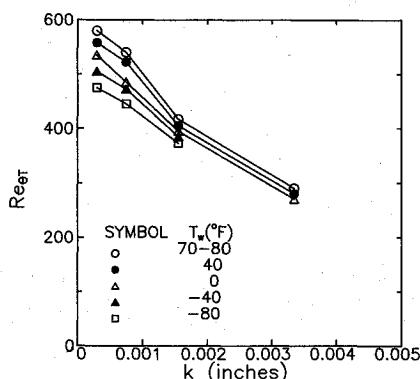


Fig. 4 Dependence of the midpoint transition Reynolds number at the sonic point, on random roughness height and wall temperature.

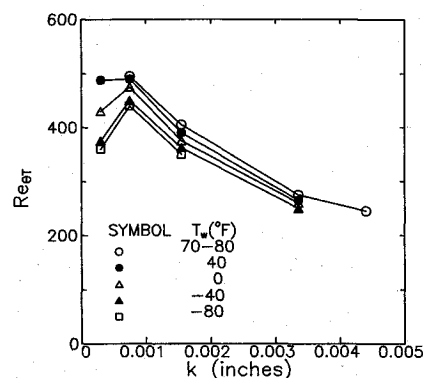


Fig. 5 Dependence of the midpoint transition Reynolds number at the supersonic side of the throat, on random-roughness height and wall temperature.

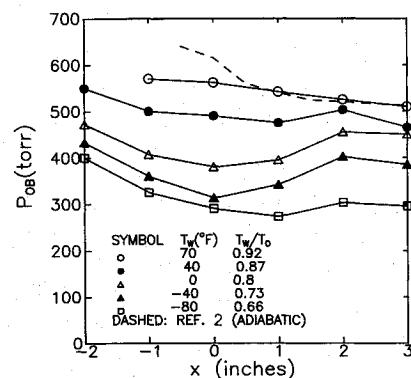


Fig. 6 Dependence of beginning-transition tunnel pressure on wall temperature (smooth wall).

ice acting as such a transition "trip." In the present experiment, excellent visibility of the complete nozzle surface upstream of the throat allowed continuous checks on ice formation throughout the tests. Surface condensation was first detected at about -50°F , and ice formation first appeared at -80°F , both long after transition began its march upstream as T_w was lowered (see Fig. 3). It was concluded that surface condensation could not explain the sensitivity of transition location to T_w .

Figure 6, whose ordinate denotes the stagnation pressure p_{0B} at which transition onset was first recorded, contains interesting information on the stability of the cooled flow. At wall temperatures of 0 and -40°F it is seen that the curves have a minimum near the sonic point; thus for certain stagnation pressures it would appear that the "turbulence" at that point is preceded and followed by laminar flow as would occur in relaminarization. Actually, the technique used only goes as far as to say that the "turbulence" was activity at specific regions of the spectrum, which activity was damped at some downstream distance. It could well be that this phenomenon, already mentioned earlier in connection with the narrowband-vs-wideband technique, is the result of a complex instability behavior of compressible boundary layers over a curved surface, with pressure gradient and heat transfer, which invites detailed study in the future.

The effect of wall cooling on transition with the sand-type random-roughness overlays in place is already evident on Figs. 4 and 5. With such roughness, transition movement and possible relaminarization or restabilization phenomena, the latter as just qualified, were evident only for low k values; as the roughness height increased, the T_w effect decreased until it was barely discernible. For these data departures from the blunt-body "correlation" of Fig. 1 were small and occurred only for the low k limit shown on the left of the figure.

Initial experiments with the etched weave-type roughness overlays featured relatively small (on the order of 2–3) ratios

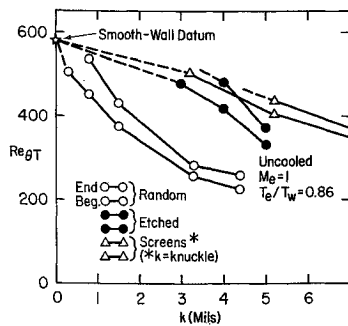


Fig. 7 The effect of roughness height k on transition Reynolds number, for three different types of roughness (adiabatic sonic conditions).

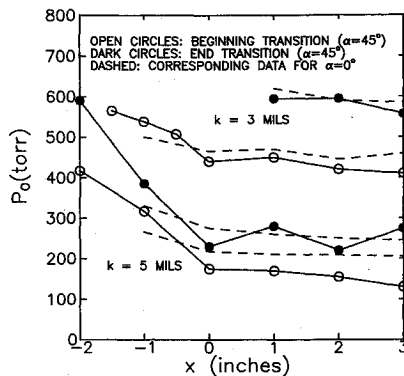


Fig. 8 Effect of wave-roughness orientation angle on the tunnel pressures at which transition was noted (adiabatic conditions).

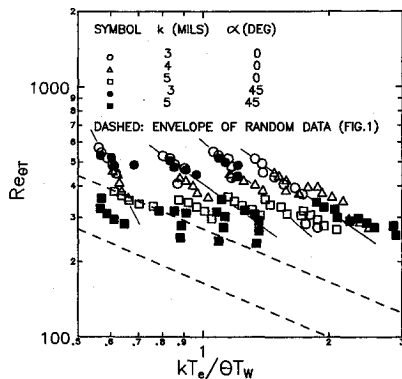


Fig. 9 The transition Reynolds numbers observed with the etched roughness, compared with the correlation of Fig. 1.

of the wavelength S to the width t of the roughness and an orientation of the pattern axes so that the incidence angle α was zero (see Fig. 2 for definitions of S , t , and α). The transition location on these overlays remained sensitive to T_w , but the location itself differed little from that with smooth walls, as shown in Fig. 7, which also shows the much greater tripping efficiency of the random (sand-type) roughness. Figure 8 shows the tunnel pressures and nozzle locations of transition obtained with the same etched patterns positioned with their major axes at $\alpha = 45$ deg incidence to the flow direction. Little difference is seen between these and the $\alpha = 0$ deg results, and at $T_w = 0.66T_0$ the results for $\alpha = 45$ deg actually give slightly higher $Re_{\theta T}$ values than those at $\alpha = 0$ deg.

Transition midpoint data obtained with the weave-type (etched-overlay) roughnesses are shown on Fig. 9, drawn in the coordinates of Fig. 1 for comparison with random roughness. The weave-type data are widely scattered, lie far from the "correlation" of Fig. 1, and show transition occurring

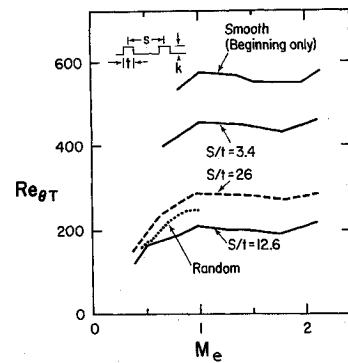


Fig. 10 Effect of weave-type roughness wavelength on the midpoint transition Reynolds number for adiabatic walls, $k = 0.004$ in. (0.01 cm).

much later than predicted from the random data; these differences persist even if Fig. 9 were to be replotted utilizing the Batt-Legner correlation of Eq. (1) with the curvature term included ($d \neq 0$). It is likely that the comparison with the random data is improper since the latter are characterized by the average k , whereas they may trigger transition only by the action of large, isolated roughness elements. The short solid lines on Fig. 9 group the data according to location on the nozzle, i.e., according to different values of M_e , pressure gradient, etc. This phenomenon, also noted by Batt and Legner in previous data, is yet unexplained.

These results also differ considerably from those reported by Laderman⁴ and Reda⁵ for periodic weave-type roughness, which in their case was an efficient transition trip. These authors, however, seem to have used surface roughness patterns that were geometrically more complex than the etched overlays used here. Furthermore, the present etched pattern was a succession of rectangular cavities on an otherwise smooth wall and thus belongs to a class of flows studied long ago by Charwat et al.¹⁶ These workers found that the laminar boundary layer over such a surface virtually ignores the existence of the cavities for the range of S/k ratios of the tests just described and thus experiences no inducement toward transition due to roughness.

On the strength of such reasoning, it was decided to minimize the distance between cavities and thus the top surface (i.e., the length t , Fig. 2) of the roughness "elements" of the etched pattern. Figure 10, which compares three such roughness overlays of the same k , shows that an increase of the S/t ratio makes the etched roughness very effective and actually more so than random roughness of the same height. Note, however, that this empirical effect is not monotonic and that in this particular case an intermediate S/t ratio ($= 12.6$) was the most effective. As one would really expect, "resonant" roughness configurations might exist where the roughness geometry provides the best conditions for tripping the layer.

Finally, screen overlay tests were conducted with the wire mesh geometries pictured on Fig. 2. These proved to be the least efficient method for tripping the layer, as already shown on Fig. 7. Data produced with these screen overlays (using k as the "knuckle" height of Fig. 2) produced transition Reynolds numbers $Re_{\theta T}$ higher by a factor of about 2, at nondimensional roughness heights $(k/\theta)(T_e/T_w) = 2$, than those observed with random roughness.

Conclusions

On the basis of the experiments reported here, the following conclusions are appropriate.

1) The boundary-layer transition data obtained in the throat region of the DeLaval nozzle employed strengthen the earlier conviction that the phenomena in that region simulate quite closely those of laminar boundary layers on blunt bodies.

2) Although roughness plays an important role in boundary-layer transition on nozzles and blunt bodies, roughness cannot by itself explain why wall cooling causes transition to move upstream. A theoretical connection between blunt surface cooling and transition is still much in demand. In view of the present observations of possible relaminarization/restabilization due to cooling, boundary-layer stability measurements in the throat region would be equally fruitful.

3) The transition data obtained with the weave-type roughness, compared with corresponding sand-type roughness data of equal height k , generally show little effect of the roughness on transition. For such weave-type roughness, existing blunt-body correlations appear invalid.

4) The present data also indicate that, first, the orientation relative to the flow vector of etched, weave-type roughness and also screen roughness is not an important factor in increasing the tripping efficiency and, second, significant changes in tripping efficiency can occur for certain wavelengths of roughness patterns such as the periodic (weave-type or screen) patterns. The latter finding would be most interesting to pursue further, by observing the transition movement caused by changes in the roughness wavelength-to-height ratio.

Acknowledgments

This work was supported by TEXTRON Defense Systems under U.S. Air Force Contract F04701-80-C-0032. The author acknowledges helpful discussions with Barry Reeves and Noel Thyson.

References

- ¹Batt, R. G., and Legner, H. H., "A Review of Roughness-Induced Nosedip Transition," AIAA Paper 81-1223, June 1981.
- ²Demetriades, A., "Roughness Effects on Boundary-Layer Transition in a Nozzle Throat," *AIAA Journal*, Vol. 19, No. 3, 1981, pp. 282-289.
- ³Anderson, A. D., "Passive Nosedip Technology (PANT) Program, Interim Report, Vol. X: Boundary-Layer Transition on Nosedips with Rough Surfaces," U.S. Air Force SAMSO, SAMSO TR-74-86, Los Angeles, CA, Jan. 1975.
- ⁴Laderman, A. J., "Effect of Surface Roughness on Blunt Body Boundary-Layer Transition," *Journal of Spacecraft and Rockets*, Vol. 14, No. 2, 1977, pp. 253-255.
- ⁵Reda, D. C., "Correlation of Nosedip Boundary-Layer Transition Data Measured in Ballistic-Range Experiments," *AIAA Journal*, Vol. 19, No. 3, 1981, pp. 329-339.
- ⁶Van Driest, E., private communications, Aerospace Corp., Los Angeles, CA, 1977-1978.
- ⁷Dirling, R. B., Jr., Swain, C. E., and Stokes, T. R., "The Effect of Transition and Boundary Layer Development on Hypersonic Re-Entry Shape Change," AIAA Paper 75-673, May 1975.
- ⁸Merkle, C. L., "Stability and Transition in Boundary Layers on Reentry Vehicle Nosedips," Flow Research Inc., Rept. No. 71 (AFOSR-TR-76-1107), Kent, WA, June 1976.
- ⁹Kuethe, A. M., "On the Stability of Flow in the Boundary Layer Near the Nose of a Blunt Body," Rand Corp., Rept. No. RM-1972, Santa Monica, CA, Aug. 1957.
- ¹⁰Ferri, A., and Vaglio-Laurin, R., "A Note on the Effect of Centrifugal Forces and Accelerated Motion on the Instability of the Laminar Boundary Layer About Highly Cooled Bodies," Polytechnic Inst. of Brooklyn, Rept. No. PIBAL 313, Brooklyn, NY, Dec. 1956.
- ¹¹Beckwith, I. E., and Holley, B. B., "Gortler Vortices and Transition in Wall Boundary Layers of Two Mach 5 Nozzles," NASA TP 1869, Aug. 1981.
- ¹²Wisniewski, R. J., "Note on a Correlation of Boundary Layer Transition Results on Highly Cooled Blunt Bodies," NASA Memo 10-8-58E, 1958.
- ¹³Krasnican, M. J., and Rabb, L., "Effects of Nose Radius and Extreme Cooling on Boundary-Layer Transition for Three Smooth 15-Deg. Cone Cylinders in Free Flight at Mach Numbers to 8.5," NASA Memo 3-4-59E, 1959.
- ¹⁴Lysenko, V. I., and Maslov, A. A., "Transition Reversal and One of Its Causes," *AIAA Journal*, Vol. 19, No. 6, 1981, pp. 705-708.
- ¹⁵Cooper, M., Mayo, E. E., and Julius, J. D., "The Influence of Low Wall Temperature on Boundary-Layer Transition and Local Heat Transfer on 2-Inch Hemispheres at a Mach Number of 4.95 and a Reynolds Number per Foot of 73.2 Million," NASA TN D-391, March 1960.
- ¹⁶Charwat, A. F., Dewey, C. F., Jr., Roos, J. N., and Hitz, J. A., "An Investigation of Separated Flows, Part II: Flow in the Cavity and Heat Transfer," *Journal of the Aeronautical Sciences*, Vol. 27, No. 7, 1961, pp. 513-527.

James E. Daywitt
Associate Editor